

Duncan P. Fagg · Vladislav V. Kharton
Jorge R. Frade

Transport in ceria electrolytes modified with sintering aids: effects on oxygen reduction kinetics

Received: 11 April 2003 / Accepted: 29 September 2003 / Published online: 23 March 2004
© Springer-Verlag 2004

Abstract Small (2 mol%) cobalt oxide additions to ceria-gadolinia (CGO) materials considerably improve sinterability, making it possible to obtain ceramics with 95–99% density and sub-micrometre grain sizes at 1,170–1,370 K. The addition of Co causes a significant shift of the electrolytic domain to lower pO_2 . This modification to the minor electronic conductivity of the electrolyte material has influence on the cathodic oxygen reduction reaction. The impedance technique is shown to provide information not only about polarisation resistance, but also about the active electrode area from analysis of the current constriction resistance. It is demonstrated that this current constriction resistance can be related to the minor electronic contributions to total conductivity in these materials. A simple imbedded grid approach gives control of the contact area allowing the properties of the electrolyte materials to be studied. A much lower polarisation resistance for the Co-containing CGO electrolyte is observed, which can be clearly attributed to an increased three-phase reaction area in the Co-containing material, as a consequence of elevated p-type conductivity.

Keywords Gadolinia-doped ceria · Electrolyte · Sintering aids · Oxygen reduction kinetics · Impedance spectroscopy

Introduction

Solid electrolytes based on doped cerium dioxide, $Ce(M)O_{2-\delta}$ (M: rare earth cations), are considered one of the most promising alternatives to yttria-stabilised zirconia (YSZ) ceramics for applications in electrochemical

devices operating at intermediate temperatures (770–970 K), due to the four–five times higher ionic conductivity of ceria-based materials in this temperature range [1, 2, 3, 4, 5, 6, 7, 8]. At temperatures below 1,000 K, electronic leakage due to reduction of Ce^{4+} to Ce^{3+} has been shown to be minimal and successful incorporation in devices such as solid oxide fuel cells (SOFCs) has been demonstrated. Recently, Kleinlogel and Gauckler [6, 7] have sintered dense Gd-substituted CeO_2 (CGO) with nano-sized grains at temperatures as low as 1,170 K by the addition of small quantities (<5 mol%) of binary transition metal oxides such as cobalt or copper oxide. The nano-sized grain structure is likely to have greater mechanical stability than conventionally processed CGO sintered at higher temperatures.

Previous results from our group [9, 10] have shown that, whilst these minor dopant additions have no essential effect on the total and ionic conductivity, the p-type conduction in the transition metal-containing materials at 900–1,200 K is 8–30 times higher than that in undoped CGO. The oxygen ion transference numbers of the Co-, Fe- and Cu-doped ceramics, determined by the modified electromotive force (EMF) technique under oxygen/air gradient, are in the range 0.89–0.99. The contribution of the electron-hole conductivity to the total conductivity increases with temperature, as the activation energy for ionic conduction, 72 to 83 kJ/mol, is significantly lower than that for the p-type electronic transport (118–176 kJ/mol). Ion-blocking results have shown the inverse result that the n-type conductivity is depleted in Co-doped CGO materials when compared to that of undoped CGO [10].

Consequently, doping with trace amounts of transition metal oxides could beneficially enhance the oxygen exchange rate in conditions where a higher electronic conductivity at the electrolyte surface would be created [11, 12]. For example, incorporation of transition metal cations into the surface layers of YSZ ceramics was shown to considerably decrease electrode polarisation [13, 14]. A similar effect was observed for 2% Pr-doped CGO, where the variable-valence Pr cations simulta-

D. P. Fagg (✉) · V. V. Kharton · J. R. Frade
Department of Ceramics and Glass Engineering, CICECO,
University of Aveiro, 3810-193 Aveiro, Portugal
E-mail: duncan@cv.ua.pt
Tel.: +351-234-370263
Fax: +351-234-425300

neously increase electron-hole transport and act as catalytically active centres [15]. Conversely, higher electronic conductivity resulting from such doping may also have a negative effect on the electrochemical cell performance. Continuing our research on CeO₂-based solid electrolytes [9, 10, 15, 16, 17], this paper studies imbedded platinum mesh electrodes on Co-free CGO and Co-CGO electrolytes to assess the influence that modifications to the minor electronic contribution will provoke on the oxygen reduction kinetics of the parent CGO material.

Materials and methods

Commercial Ce_{0.80}Gd_{0.20}O_{2-δ} powder (Rhodia, Germany) with crystallite size of 20 nm and specific surface area of about 26 m²/g was used as the starting material to which 2 mol% cobalt oxide was added in the form of nitrate, Co(NO₃)₂·6H₂O (Merck, Germany). Note that the starting Ce_{0.80}Gd_{0.20}O_{2-δ} (CGO) powder, used in this work, is the same as that used by Kleinlogel and Gauckler [6, 7], who also employed the nitrate method to introduce transition metal dopants into the ceria solid electrolyte.

A stoichiometric amount of an aqueous solution of the dopant nitrate was added to the CGO powder and mixed well. After drying, the powder was milled in an agate mortar and dry-pressed into pellets (diameter of 30 mm, pressure of about 30 MPa). Phase composition was determined by X-ray diffraction (XRD) using a Rigaku Geigerflex diffractometer (CuK_α radiation). No evidence of secondary phases was discernible by XRD. Trace electron-hole conductivity was separated from total electrical conductivity [9] using the modified EMF method proposed by Gorelov [18], whilst the ion blocking technique [16] was used to separate the n-type conductivity [10]. Co-containing CGO is hereafter designated Co-CGO.

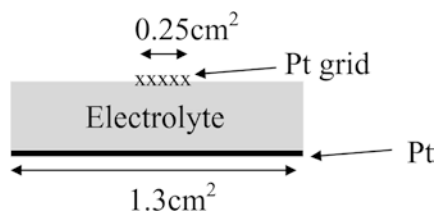
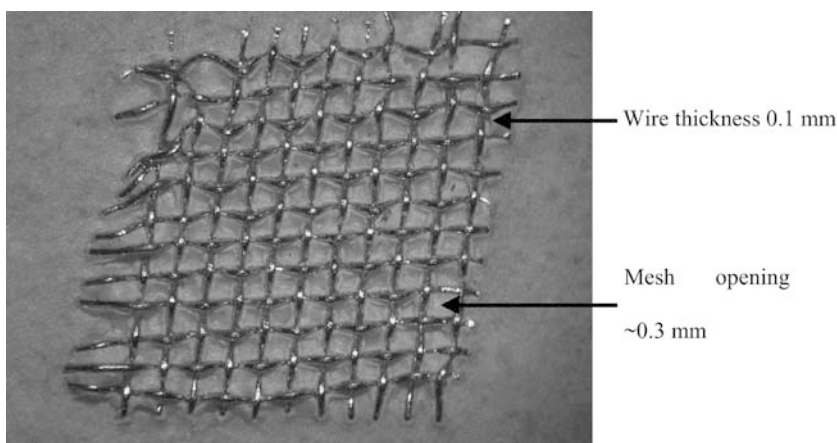


Fig. 1 Schematic of electrolyte and electrode layers, showing overall cell geometry

Fig. 2 Optical microscope image of Pt grid imbedded into CGO electrolyte surface. Geometric appearance of imbedded Pt grid in Co-containing CGO electrolyte is equivalent



Impedance analysis was performed using the Autolab ECO Chimie B.V. frequency response analyser in the frequency range 0.5 MHz–0.1 Hz with amplitude 50 mV. Impedance spectra were fitted using the Scribner Zview program. Overpotential values (η) were calculated by the equation $\eta = V - I(R_1 + R_2)$ where V is the applied potential, R_1 describes the ohmic resistance of the electrolyte material, and R_2 accommodates the additional ohmic electrolyte resistance which arises due to a frequency dependent potential distribution, as explained below.

Results and discussion

Electrode microstructure

The sample cell is described schematically in Fig. 1, whilst Fig. 2 shows an optical microscope image of the platinum mesh electrode imbedded into the CGO electrolyte surface. The geometric appearance of the imbedded mesh electrode in Co-CGO electrolyte is equivalent.

The three-phase contact length (TPB) between the gaseous phase, an electronically conducting phase and an ionically conducting phase is a factor of utmost importance when studying electrode reaction kinetics. Unfortunately, the length of the TPB is also a factor that is extremely difficult to measure accurately for a real system. For example in the study of cermet-type electrode materials the three-phase boundary length is normally estimated by either chemical means, such as the BET method [19], or by basic microscopic analysis. To avoid this complexity many authors have adopted simplified approaches for the study of cermet electrodes, in which the granular, ionically conducting matrix is omitted, thereby reducing the three-dimensional microstructure to a two-dimensional one. Examples of this type of approach are that of point electrode or pattern electrode studies [20, 21, 22]. In this work we aimed to qualitatively compare the influence that two compositionally different electrolyte materials have on electrode kinetics. What is imperative for this experimental aim, therefore, is a high degree of control of the TPB length. The use of an imbedded Pt grid offers a neat method of achieving this prerequisite. In the study of each electrolyte material

the overall cell geometry is kept constant as described in Fig. 1; this includes the total grid area and also the sample pellet size. From Fig. 2, one can see that the imbedded grid provides contact solely at its lowest points and the number of these points is both finite and can also be considered equal for the two electrolyte materials. For this reason, and to a good approximation, one can state that the geometrical contact area for the Co-CGO and the CGO samples can be considered constant.

Impedance spectra and the equivalent circuit

Typical impedance spectra of these samples are shown in Fig. 3a, b. The example presented is for the CGO material under cathodic polarisation of -0.4 V at 600 °C. The insert of Fig. 3a expands the scale at high frequency revealing an offset along the real Z' -axis and also shows results for Co-containing CGO. An asymmetric response can also be observed at lower frequencies both in the complex plane plot, Fig. 3a and also

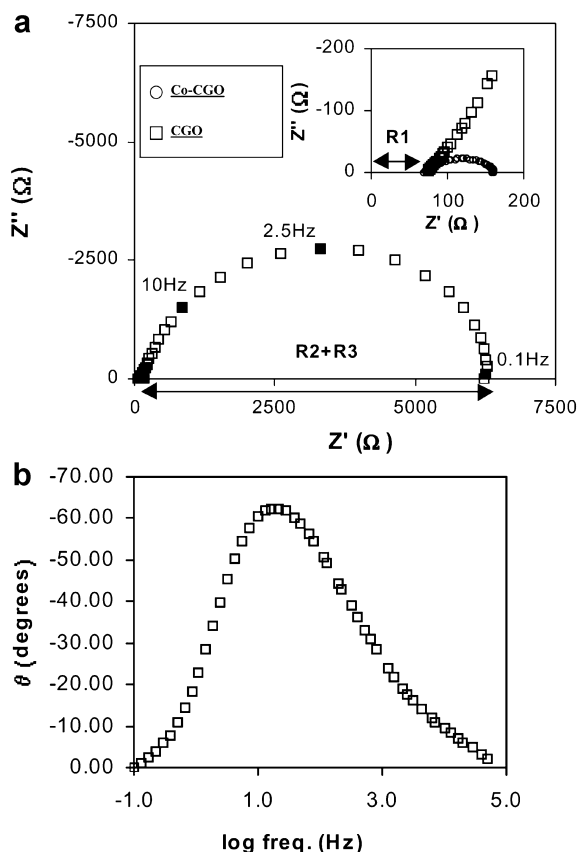


Fig. 3a, b Typical impedance spectra showing asymmetry. The main spectrum in **a** is that of an imbedded Pt-grid on ceria-gadolinia (CGO) electrolyte under cathodic polarisation, -0.4 V at 600 °C. The asymmetry is more apparent when data is plotted in form of phase angle against frequency (**b**). *Inset* in **a** magnifies the offset at high frequency along real Z' axis, correspondent to the value of the ohmic resistance of the electrolyte material (R_1), and presents results for an imbedded Pt-grid on Co-containing CGO under the same conditions

more clearly in the bode plot of phase angle against frequency, Fig. 3b. This asymmetry dictates that more than one process is occurring within the lower frequency range. Modelling of impedance spectra was performed using an equivalent circuit suggested by many authors such as Gauckler [20] and Maier [23] and presented in Fig. 4. The physical meaning of each element is as follows. The element R_1 represents the ohmic resistance of the electrolyte material, whilst R_2 accommodates the additional ohmic electrolyte resistance which arises due to a frequency dependent potential distribution. This term is commonly called the current constriction resistance [23, 24]. Accommodation of charge transfer occurring at the electrode/electrolyte interface is simply attempted by the parallel combination of a constant phase element CPE3 and R_3 . Extension of the TPB away from that of the geometric points of contact of the imbedded grid and the electrolyte surface, for example by an enhanced electronic conductivity in the electrolyte material, would be thought to lower the current constriction resistance R_2 due to an enlargement of reaction surface area. Average percentage error values from the fit of variables are shown in Table 1.

The physical significance of R_1 , R_2 and R_3

The value of R_1 is shown by Fig. 5 to be comparable for the Co-containing and Co-free electrolyte materials and to be independent of overvoltage. The hypothesis that R_1 represents the electrolyte resistance is confirmed by observing its temperature dependence, Fig. 5a. The calculated activation energy of 79 kJ/mol corresponds well with literature data for the total conductivity of these materials in air [9, 10]. In Fig. 6a the values of R_2 for the CGO material are presented. In contrast to those exhibited by R_1 , the R_2 values are shown to be overpotential-dependent and to go through maxima at inter-

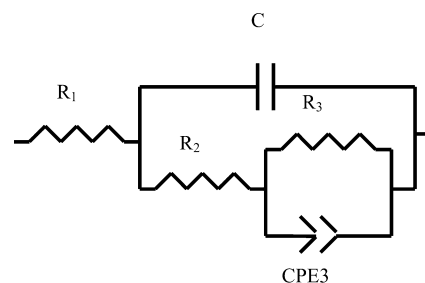


Fig. 4 Equivalent circuit model. R_3 Polarisation resistance, CPE3 constant phase element. R_2 Additional ohmic electrolyte resistance which arises due to a frequency-dependent potential distribution, Co-CGO Co-containing CGO

Table 1 Average error values from fit of variables

Variable	R_1	C	R_2	Q_3 (CPE3)	N	R_3
Average error (%)	1.5	11	10	6	1.5	2

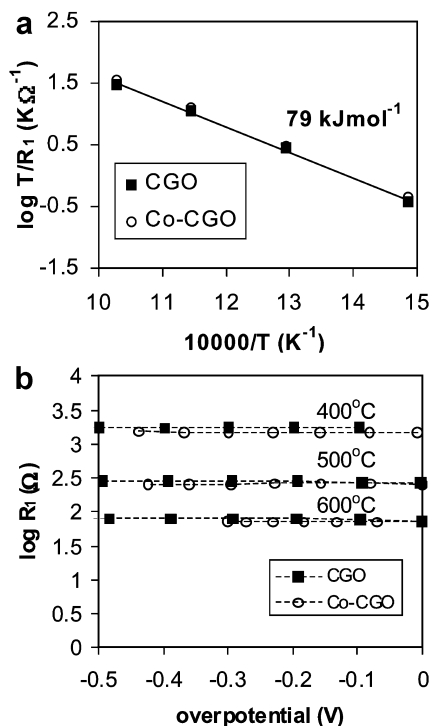


Fig. 5 **a** Temperature dependence of R_1 for imbedded Pt grids on Co-CGO and CGO electrolytes yielding activation energies for conduction equal to 79 kJ/mol. **b** Overpotential dependence of R_1 for imbedded Pt grids on Co-CGO and CGO electrolytes at different temperatures. Values of R_1 for Co-CGO and CGO materials are equivalent

mediate values of overpotential. The exact locations of the maxima are shifted to lower values of overpotential as temperature increases. To explain this phenomenon one must look to the minor electronic contributions to conductivity. Figure 7 summarises data from [9, 10] for the CGO electrolyte. Experimental n-type conductivities obtained by ion-blocking measurements are plotted together with p-type conductivity values measured at corresponding temperatures by the EMF technique in an oxygen/air potential gradient. The p-type conductivities are extrapolated to lower values of pO_2 by assuming $\sigma_p \propto pO_2^{+1/4}$. Figure 7a clearly demonstrates that the pO_2 values corresponding to the electronic conductivity minima are shifted to higher pO_2 as temperature increases, whilst Fig. 7b shows that these pO_2 values are linearly dependent on temperature. This linear dependency allows the location of the electronic conductivity minima to be extrapolated to lower temperatures. The pO_2 values corresponding to the location of the minima for the temperatures 400, 500, 600 and 700 °C are listed in Table 2. The potentials associated with these pO_2 values are calculated from the Nernst equation, as shown in Table 2, and are superimposed on Fig. 6a. A good agreement between the location of the minima for electronic conductivity and the maxima for the values of R_2 is observed, suggesting a strong link between the minor electronic conductivities of these materials and the values of R_2 obtained. The physical meaning of R_2

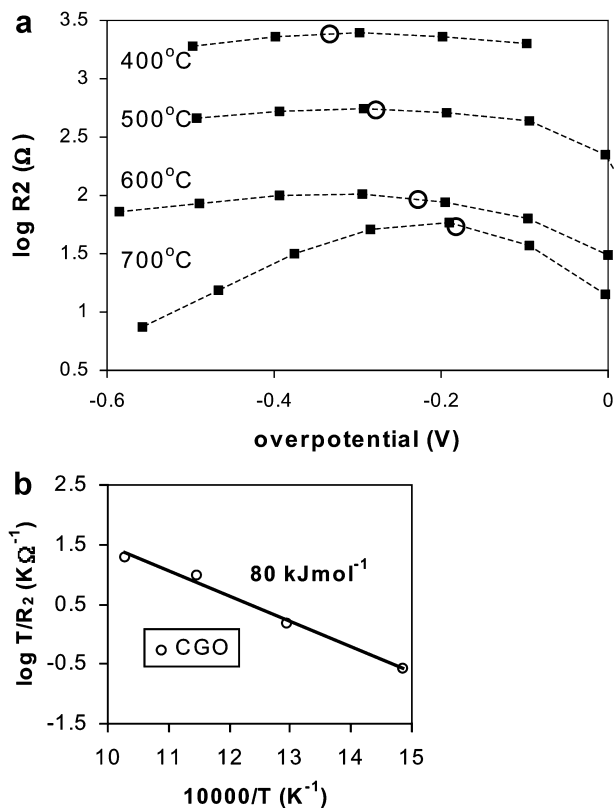


Fig. 6 **a** The overpotential dependence of R_2 for imbedded Pt grids on CGO electrolytes at different temperatures. Circles Location of the respective minima in electronic conductivity from Fig. 7a, 7b. **b** The temperature dependence of the circled R_2 values

was suggested above to be that of the additional ohmic resistance of the electrolyte due to a frequency dependent potential distribution. It was also suggested that the active electrode area may be increased if the electronic conductivity of the electrolyte surface were increased, which in turn would lead to a decrease in the magnitude of R_2 . The results do indeed support this suggestion, but in order to test this hypothesis further, one would like to confirm that R_2 is indeed an electrolyte property by observing its temperature dependence, in a similar way to that done in Fig. 5 for R_1 . However, this test would only be true if the active electrode area were temperature independent. In our case the test is complicated by the fact that the electronic transport number t_e measured for CGO [9, 10] is shown to have temperature dependence. To circumvent this complication the temperature dependence of R_2 is assessed for values of R_2 corresponding to the maxima at each temperature, which in turn correspond to the minimum values of the electronic conductivity, in other words the values of R_2 at which t_e will be minimum. This temperature dependence is plotted in Fig. 6a and gives an activation energy for conduction of 80 kJ/mol, a value which reinforces the hypothesis that R_2 is a bulk electrolyte property.

Small changes in atmosphere can reinforce the link between the value of R_2 and the minor electronic contributions to total conductivity. Figure 8 compares the

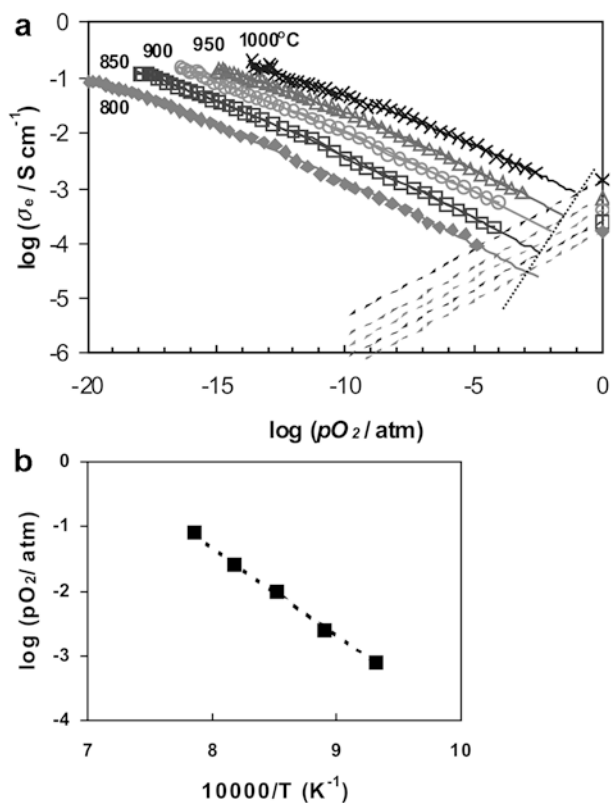


Fig. 7 a The n- and p-type electronic conductivities of CGO. b The temperature dependence of pO_2 values corresponding to the electronic conductivity minima. The n-type conductivity was measured by ion blocking measurements [10], and p-type conductivity was measured by the electromotive force (EMF) technique under an oxygen/air gradient [9] and extrapolated to lower values of pO_2 by adopting a typical dependence $\sigma_p \propto pO_2^{+1/4}$

Table 2 The pO_2 values corresponding to the minima in σ_e and their respective Nernst potentials calculated by extrapolation of the linear temperature dependence exhibited in Fig. 7b

Temperature	$\log pO_2^a$	Potential
°C	atm	V
700	-4.5	-0.18
600	-6.1	-0.23
500	-8.1	-0.28
400	-10.7	-0.34

^a σ_e minima

cathodic polarisation behaviour of the Co-free CGO sample in air and Ar atmospheres. Although the value of R_1 calculated in each atmosphere remains constant, the value of R_2 is shown to differ between the gas atmospheres. It can be observed that, whilst the overall shape of the overpotential dependence of R_2 and the maximum R_2 value remain similar, the maxima in R_2 are shifted to slightly less negative values of overpotential in the Ar case. This can be related to the minor electronic contribution to total conductivity. The Ar atmosphere provides a lower oxygen partial pressure from which to initiate cathodic polarisation. Subsequently, by reference

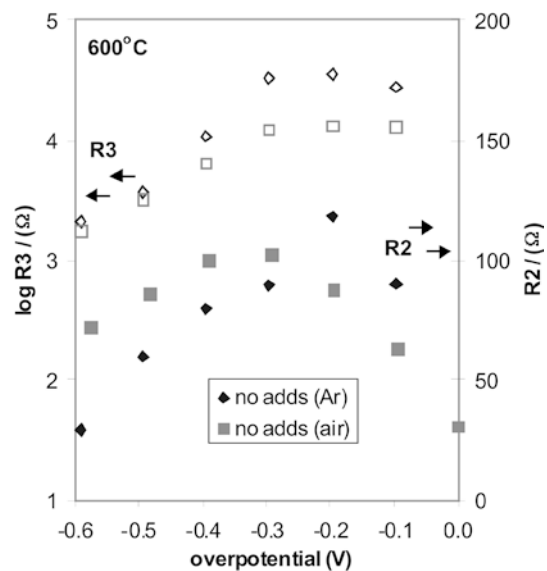


Fig. 8 The behaviour of R_2 and R_3 measured for an imbedded Pt grid on CGO electrolyte in air and Ar atmospheres. Closed symbols R_2 values, open symbols R_3 values

to Fig. 7, one can envisage that the minimum of electronic conductivity (i.e. the maximum in R_2) would be reached at smaller applied potentials in the Ar case, as confirmed in Fig. 8. This is in turn reflected by the larger values of the polarisation resistance, R_3 , obtained at small overpotential values for the Ar case, Fig. 8.

In summary, whilst both R_1 and R_2 are demonstrated to be electrolyte properties, R_1 is effectively constant between the differing electrolyte materials, overpotentials and atmospheres tested, whereas the values of R_2 are shown to be influenced. The constant values of R_1 suggest that the total bulk conductivities of the electrolyte materials remain effectively constant. On the other hand, the changing values of R_2 are shown to be interlinked with the behaviour of the minor electronic contributions to total conductivity and to influence the values of the polarisation resistance R_3 obtained.

The effect of electrode surface area

The influence of electrode surface area can be simply assessed by overpainting the platinum grid with porous Pt paint. By such an approach the active area of the working electrode will be extended from that of localised points of contact to the total geometrical grid area. Figure 9 demonstrates the effect that this increase in electrode surface area will have on the factors R_2 , R_3 , and the overall polarisation behaviour for a sample of CGO. The value of R_1 for the grid and the grid overpainted with Pt paint remains effectively constant. However, as shown in Fig. 9a, the value for R_2 is decreased dramatically for the sample that has been overpainted, whilst the general shape of the dependence of R_2 on overpotential is maintained. This observation

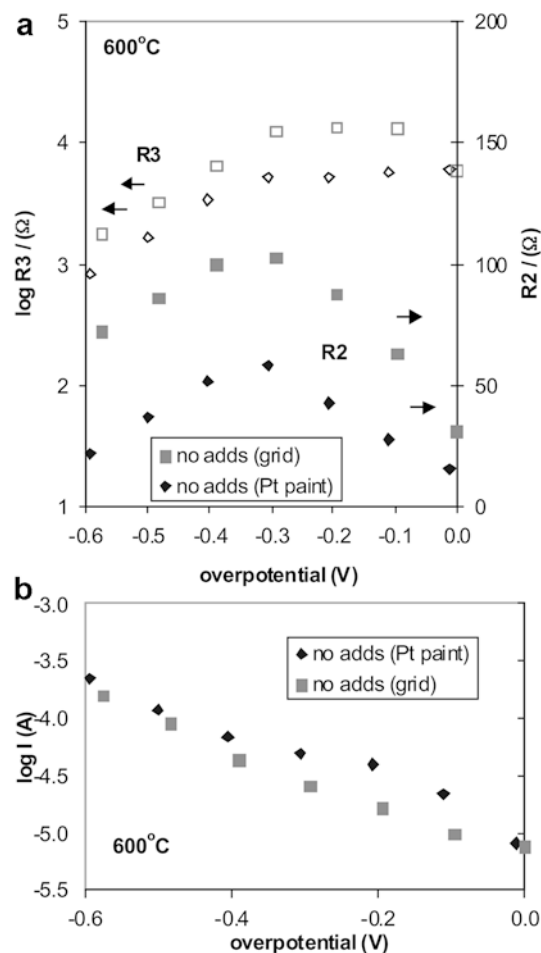


Fig. 9a, b The overpotential dependence of R_2 and R_3 (a) and current (b) for an imbedded Pt grid on CGO electrolyte compared to the same sample with the grid area overpainted with porous Pt paint. Closed symbols R_2 values, open symbols R_3 values

again reinforces the suggestion that R_2 , the current constriction resistance, is a bulk electrolyte property that gives an indication of the active electrode surface area. As the active surface area is increased, the magnitude of R_2 is decreased. This increase in active surface area for reaction subsequently leads to a decrease in the polarisation resistance, R_3 (Fig. 9a). The polarisation resistance, R_3 , measured for the grid overpainted with Pt paint is observed to be much lower than that for the unpainted grid in the intermediate overpotential range. This leads to improved polarisation behaviour in the same region (Fig. 9b). From the discussion of the previous section this intermediate overpotential range corresponds to the lowest electronic transport. For the unpainted sample the active electrode surface area can be suggested localised at the points of contact between the grid and the electrolyte surface when the electronic conductivity is low. Within this region of low electronic conductivity R_2 and R_3 are shown to be large with respect to the values shown for the overpainted sample of larger active electrode surface area.

The comparison of Co-containing and Co-free materials

As mentioned above, the values of R_1 measured for the Co-CGO and CGO electrolyte materials are effectively constant. However, the calculated value of R_2 is radically decreased in the case of the Co-containing CGO electrolyte, Fig. 10a. In the previous sections the physical significance of the current constriction resistance, R_2 , was demonstrated. The magnitude of R_2 was shown to supply information about the active electrode surface area and to have its root in the level of the electronic contribution to total conductivity. Reference to Fig. 10a, therefore, allows the lower values of current constriction resistance, R_2 , measured in the Co-CGO case, to suggest a larger active electrode surface area with respect to that in Co-free CGO. Furthermore this larger active surface area for reaction should be related to the electronic contribution to total conductivity. Figure 11 compares the minor electronic conductivities of Co-CGO to that of Co-free CGO, and is obtained in the same way as that described for Fig. 7. Although the n-type conductivity is slightly suppressed in Co-CGO compared to CGO, it is observed that the p-type conductivity is substantially enhanced. It is suggested that this enhanced p-type conductivity allows electrode reaction to occur over an area much greater than that possible in the Co-free CGO case. It should be stated that the values of R_2 obtained for the Co-CGO sample do not show a significant overpotential dependence unlike the case of Co-free CGO. This could be as a result of the much smaller values of R_2 in the Co-CGO case. An average 10% fitting error in the values of R_2 , (Table 1), may become more significant when changes in R_2 become small. The asymmetric counter-working electrode design is beneficial not only due to the increased current density at the working electrode and therefore the ease of assignment of R_3 , but also because it gives a current constriction resistance in addition to that which arises solely from the grid. This additional current restriction resistance enhances the ease of resolution of R_2 . Unfortunately this is not the case when the active electrode area approaches that of total grid area. The additional current constriction resistance stemming from the asymmetric counter-working electrode design may indeed disguise the much smaller current restriction resistance originating from effects related to the grid.

Supporting the hypothesis that the active electrode surface area increases with Co additions, is the value of capacitance; for a larger electrode surface area the capacitance should be increased. Figure 10b plots the overpotential dependence of C_3 , (calculated from $C_3 = R_3^{(1-n)/n} Q_3^{1/n}$, where Q_3 is the constant phase element CPE3, and n is the deviation of the impedance of the CPE from an ideal capacitor) for the samples Co-CGO and CGO with the Pt grid and the Pt overpainted grid. The capacitance values of C_3 follow the expected trend well. Both samples of expected larger active electrode surface area, Co-CGO and also CGO with the

Fig. 10a–d The overpotential dependence of R_2 (a), C_3 (b), R_3 (c) and current (d) for an imbedded Pt grid on CGO electrolyte compared to that of Co-CGO. In Fig. 10a, *Open symbols* Co-CGO, *closed symbols* CGO, *circles* 400 °C, *triangles* 500 °C, *squares* 600 °C

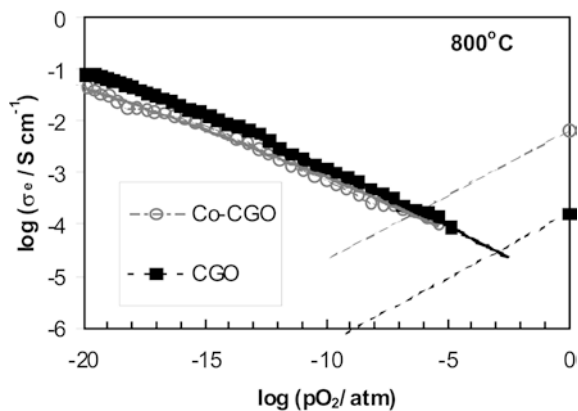
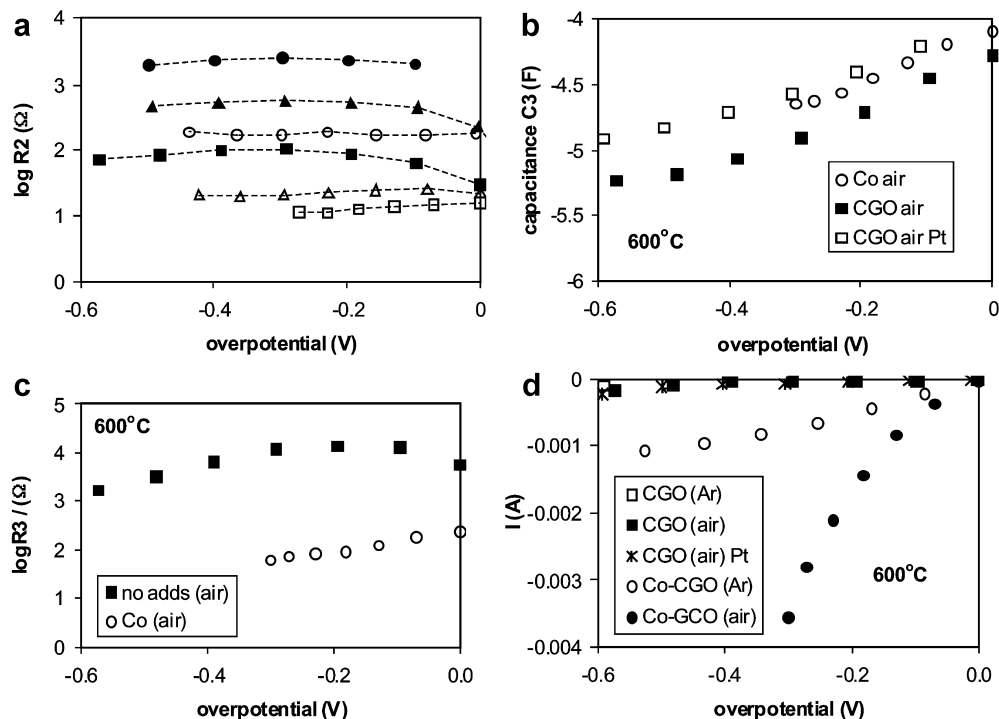


Fig. 11 The n-type conductivities obtained by ion blocking measurements [10], plotted together with p-type conductivity values measured by the EMF technique [9] of the Co-containing CGO electrolyte, compared to that of CGO. The p-type conductivities are extrapolated to lower values of $p\text{O}_2$ by adopting a typical dependence $\sigma_p \propto p\text{O}_2^{+1/4}$

Pt-grid overpainted with Pt paste, exhibit larger C_3 values than that of the unpainted Pt grid on CGO. The values of C obtained by fitting to the equivalent circuit shown in Fig. 4 give capacitance values typically an order of magnitude lower than that of C_3 in the order of 1×10^{-6} F. No such distinct trends can be observed for C , perhaps due to its small magnitude and subsequently higher average percentage errors as shown in Table 1.

Following from the decrease in the magnitude of R_2 related to an increase in active electrode surface area, the value of the polarisation resistance, R_3 , is much lower in the case of Co-CGO than that of CGO (Fig. 10c). Correspondingly the polarisation behaviour of Co-CGO

is substantially improved when compared to that of CGO (Fig. 10d).

In conclusion, the impedance technique is shown to powerfully provide information not only about polarisation resistance but also to provide information about the active electrode area from analysis of the current constriction resistance. It has been demonstrated that this current constriction resistance can be related to minor electronic contributions to total conductivity for these materials and that a simple imbedded grid approach can give control of TPB length, allowing the properties of electrolyte materials to be studied.

Although additions of the sintering aids are small, the p-type electronic conductivity of CGO ceramics significantly increases on the addition of 2 mol% Co. This enhancement in p-type conductivity has a dramatic effect on the oxygen reduction kinetics. An enlargement of the active electrode surface area is caused by the elevated electronic conductivity and this leads to a substantial improvement in polarisation behaviour. The importance of this finding should not be understated, as one of the major drawbacks of typical cermet material structure remains that of current distribution, especially when used on thin electrolytes.

Acknowledgements This work was supported by the FCT, Portugal (PRAXIS program and the contracts SFRH/BPD/3529/2000 and POCTI/CTM/39381/2001).

References

1. Steele BCH (2000) Solid State Ionics 129:95
2. Huijsmans JPP (2001) Curr Opin Solid State Mater Sci 5:317

3. Yamamoto O (2000) *Electrochim Acta* 45:2423
4. Christie GM, van Berkel FPF (1996) *Solid State Ionics* 83:17
5. Hong SJ, Mehta K, Virkar AV (1998) *J Electrochem Soc* 145:638
6. Kleinlogel C, Gaukler LJ (1999) Nano sized ceria solid solutions for intermediate temperature solid oxide fuel cells. In: Singhal SC and Dokiya M (eds) 6th Int Symp of Solid Oxide Fuel Cells (SOFC VI) PV99–19. The Electrochemical Society, Pennington, N.J., p 225
7. Kleinlogel C, Gauckler LJ (2000) *Solid State Ionics* 135:567
8. Tianshu Z, Hing P, Huang H, Kilner J (2001) *Mater Sci Eng B* 83:235
9. Fagg DP, Kharton VV, Frade JR (2002) *J Electroceram* 9:199
10. Fagg DP, Abrantes JCC, Coll DP, Núñez P, Kharton VV, Frade JR (2003) *Electrochim Acta* 48:1023
11. Kharton VV, Naumovich EN, Vechev AA (1999) *J Solid State Electrochem* 3:61
12. Steele BCH, Hori KM, Uchino S (2000) *Solid State Ionics* 135:445
13. Bohac P, Orliukas A, Gauckler LJ (1995) Lowering of the cathode overpotential of SOFC by electrolyte doping. In: Waser R (ed) Proc Int Conf “Electroceramics IV”, vol. 2. Augustinus Buchhandlung, Aachen, p.771
14. Thampi KR, McEvoy AJ, Van herle J (1995) *J Electrochem Soc* 142:506
15. Kharton VV, Figueiredo FM, Navarro L, Naumovich EN, Kovalevsky AV, Yaremchenko AA, Viskup V, Carneiro A, Marques FMB, Frade JR (2001) *J Mater Sci* 36:1105
16. Navarro LM, Marques FMB, Frade JR (1997) *J Electrochem Soc* 144:267
17. Mather GC, Fagg DP, A.Ringuedé A, Frade JR (2001) *Fuel Cells* 1:1
18. Gorelov VP (1988) *Elektrokhimiya* 24:1380 (in Russian)
19. Sasaki K, Wurth J-P, Gschwend R, Gödickemeier M, Gauckler LJ (1996) *J Electrochem Soc* 143:530
20. Bieberle A, Meier LP, Gaukler LJ (2001) *J Electrochem Soc* 148(6):A646
21. Gharbage B, Marques FMB, Frade JR (2000) *Solid State Ionics* 136/137:933
22. Lauret H, Hammou A (1996) *J Eur Ceram Soc* 16:447
23. Fleig J, Pham P, Sztulzaft P, Maier J (1998) *Solid State Ionics* 113:739
24. Fleig J, Maier J (1997) The influence of inhomogeneous potential distributions on the electrolyte resistance in solid oxide fuel cells. In: Stimming U, Singhal SC, Tagawa H, Lehnert W (eds) Proc 5th Int Symp on Solid Oxide Fuel Cells, PV 97–40. Aachen, Germany, p 1374